Overall Water Splitting on $(Ga_{1-x}Zn_x)(N_{1-x}O_x)$ Solid Solution Photocatalyst: Relationship between Physical Properties and Photocatalytic Activity

Kazuhiko Maeda,[†] Kentaro Teramura,[†] Tsuyoshi Takata,[†] Michikazu Hara,[‡] Nobuo Saito,[§] Kenji Toda,[⊥] Yasunobu Inoue,[§] Hisayoshi Kobayashi,[||] and Kazunari Domen*[,†]

Department of Chemical System Engineering, The University of Tokyo, 7-3-1 Hongo, Bunkyo-ku, Tokyo 113-8656, Japan, Chemical Resources Laboratory, Tokyo Institute of Technology, 4259 Nagatsuta, Midori-ku, Yokohama 226-8503, Japan, Department of Chemistry, Nagaoka University of Technology, Nagaoka 940-2188, Japan, Graduate School of Science and Technology, Niigata University, 8050 Ikarashi, Ninocho, Niigata 950-2181, Japan, and Department of Chemistry and Materials Technology, Faculty of Engineering and Design, Kyoto Institute of Technology, Goshokaido-cho, Matsugasaki, Sakyo-ku, Kyoto 606-8585, Japan

Received: June 28, 2005; In Final Form: August 17, 2005

The physical and photocatalytic properties of a novel solid solution between GaN and ZnO, $(Ga_{1-x}Zn_x)(N_{1-x}O_x)$, are investigated. Nitridation of a mixture of Ga_2O_3 and ZnO at 1123 K for 5−30 h under NH_3 flow results in the formation of a $(Ga_{1-x}Zn_x)(N_{1-x}O_x)$ solid solution with $x = 0.05-0.22$. With increasing nitridation time, the zinc and oxygen concentrations decrease due to reduction of ZnO and volatilization of zinc, and the crystallinity and band gap energy of the product increase. The highest activity for overall water splitting is obtained for $(Ga_{1-x}Zn_x)(N_{1-x}O_x)$ with $x = 0.12$ after nitridation for 15 h. The crystallinity of the catalyst is also found to increase with increasing the ratio of ZnO to Ga_2O_3 in the starting material, resulting in an increase in activity.

1. Introduction

In recent years, photocatalytic materials that function under visible light have been studied extensively in an attempt to improve solar energy conversion and reduce the environmental impact of energy production. Overall water splitting using a heterogeneous photocatalyst is an attractive solution for the production of H_2 as a clean and recyclable energy source. Although a number of visible-light-driven photocatalysts have been proposed as potential candidates for overall water splitting, a satisfactory material has yet to be devised.[1−7]

The present authors recently presented a brief report on the modification of typical metal (oxy)nitrides, β-Ge_3N_4, and a solid solution of GaN and ZnO (represented as $(Ga_{1-x}Zn_x)(N_{1-x}O_x)$) with RuO_2 nanoparticles to achieve functionality as photocatalysts for overall water splitting.[8,9] In contrast to β-Ge_3N_4, which only functions under ultraviolet (UV) irradiation due to its large band gap energy (ca. 3.8 eV), $(Ga_{1-x}Zn_x)(N_{1-x}O_x)$ can decompose water under visible light. This solid solution represents the first successful example of overall water splitting using a photocatalyst with a band gap in the visible-light region (<3 eV).[9] $(Ga_{1-x}Zn_x)(N_{1-x}O_x)$ is a yellow powder that is obtained by nitriding a mixture of Ga_2O_3 and ZnO under NH_3 flow, and has a wurtzite crystal structure.

The photocatalytic activity of conventional metal-oxide photocatalysts for overall water splitting is known to be heavily dependent on the crystallinity and particle size of the material, as determined by the preparation conditions.[10−12] Therefore, investigating the physical factors that govern photocatalytic activity is an important and indispensable issue in the development of highly active photocatalysts. However, the factors affecting the photocatalytic activity of non-oxide photocatalysts for overall water splitting have yet to be investigated.

In this paper, the physicochemical properties of $(Ga_{1-x}Zn_x)(N_{1-x}O_x)$ and optimal preparation conditions are investigated in an attempt to improve the activity of this material for overall water splitting. The effects of the nitridation conditions and the ratio of ZnO to Ga_2O_3 in the starting material are examined in detail, and the factors affecting the photocatalytic activity of $(Ga_{1-x}Zn_x)(N_{1-x}O_x)$ are discussed on the basis of structural analyses.

2. Experimental Section

2.1. Preparation of $(Ga_{1-x}Zn_x)(N_{1-x}O_x)$ Solid Solution. The $(Ga_{1-x}Zn_x)(N_{1-x}O_x)$ solid solution was prepared by heating a mixture of Ga_2O_3 (High Purity Chemicals, 99.9%) and ZnO (Kanto Chemicals, 99%) powders (ca. 2 g) at 1123 K under NH_3 flow (250 mL/min). The molar ratio of Zn to Ga (Zn/Ga) in the starting material (ZnO and Ga_2O_3) was varied between 0.25 and 1.5. After 5−30 h of nitridation, the sample was cooled to room temperature under NH_3 flow.

2.2. Modification with RuO_2 Nanoparticles. RuO_2 nanoparticles were loaded onto the as-prepared $(Ga_{1-x}Zn_x)(N_{1-x}O_x)$ catalysts as a cocatalyst for H_2 evolution according to the method described previously.[12] Briefly, the $(Ga_{1-x}Zn_x)(N_{1-x}O_x)$ powder was immersed in a tetrahydrofuran (THF) solution containing dissolved $Ru_3(CO)_{12}$ (Aldrich Chemical Co., 99%) followed by stirring at 333 K for 5 h. The solution was then dried under reduced pressure by heating in air at 373 K for 1 h to remove THF. The resulting powder was finally heated in air at 623 K

* To whom correspondence should be addressed. Present address: Department of Chemical System Engineering, The University of Tokyo, 7-3-1 Hongo, Bunkyo-ku, Tokyo 113-8656, Japan. Phone: +81-3-5841-1148. FAX: +81-3-5841-8838. E-mail: domen@chemsys.t.u-tokyo.ac.jp.
† The University of Tokyo.
‡ Tokyo Institute of Technology.
§ Nagaoka University of Technology.
⊥ Niigata University.
|| Kyoto Institute of Technology.

10.1021/jp053499y CCC: $30.25
Published on Web 10/01/2005

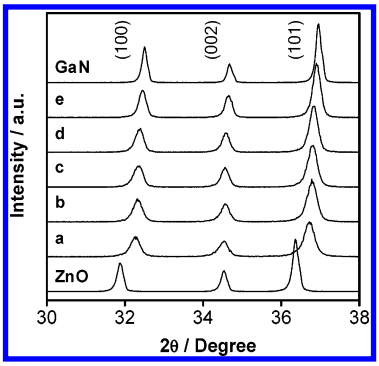

Figure 1. Powder XRD patterns of obtained samples by nitriding a mixture of Ga_2O_3 and ZnO (molar ratio Zn/Ga = 1) under a flow of NH_3 at 1123 K for (a) 5, (b) 10, (c) 15, (d) 20, and (e) 30 h. ZnO and GaN as references were purchased from Kanto Chemicals and Mitsubishi Chemicals Co., respectively.

for 1 h to convert the Ru species to RuO_2. The effective RuO_2 loading was 5 wt %.

2.3. Characterization of Catalysts. The prepared samples were studied by powder X-ray diffraction (XRD; Rigaku RINT2500HR-PC; Cu Kα), scanning electron microscopy (SEM; Hitachi S-4700), transmission electron microscopy (TEM; JEOL JEM-2010F), energy-dispersive X-ray spectroscopy (EDX; Horiba Emax-7000), UV−visible diffuse reflectance spectroscopy (DRS; Jasco V-560), and X-ray photoelectron spectroscopy (XPS; Shimadzu ESCA-3200). The binding energies determined by XPS were corrected in reference to the $Au4f_{7/2}$ peak (83.8 eV) for each sample. The Brunauer, Emmett, Teller (BET) surface area was measured with a Coulter SA-3100 instrument at liquid nitrogen temperature.

2.4. Photocatalytic Reactions. The reactions were carried out in a Pyrex inner irradiation-type reaction vessel connected to a glass-closed gas circulation system. The reaction was performed in an aqueous H_2SO_4 solution (pH 3) containing 0.3 g of the RuO_2-loaded sample. The present photocatalyst was shown previously to exhibit the highest activity for overall water splitting at pH 3.[9] The reactant solution was evacuated several times to remove air completely, followed by irradiation under a 450 W high-pressure Hg lamp ($\lambda > 300$ nm). For visible-light irradiation ($\lambda > 400$ nm), a Pyrex tube filled with sodium nitrite aqueous solution was inserted between the lamp and sample to block UV light.[9] The dependence of the activity on the wavelength of the incident light and the apparent quantum efficiency were measured with use of a top irradiation-type reaction vessel made of Pyrex and a 300 W xenon lamp with a cutoff filter. The apparent quantum efficiency (Φ) was estimated by using the following equation.

$$\Phi(\%) = \frac{\text{no. of reacted electrons}}{\text{no. of incident photons}} \times 100$$

$$= \frac{\text{no. of evolved } H_2 \text{ molecules} \times 2}{\text{no. of incident photons}} \times 100$$

Here, Φ is the apparent quantum efficiency, where it is assumed that all incident photons are absorbed by the reaction system. The number of incident photons (4.63×10^{20} photons·h^{-1} at $420 < \lambda < 440$ nm) was measured by using a Si photodiode. The evolved gases were analyzed by gas chromatography.

3. Results and Discussion

3.1. Crystal Structure and Electron Microscopy. Figure 1 shows the XRD patterns for samples obtained by nitriding a mixture of Ga_2O_3 and ZnO (molar ratio Zn/Ga = 1) at 1123 K for several periods. GaN and ZnO data are shown for comparison. A single hexagonal wurtzite phase similar to the GaN and ZnO was obtained for all prepared samples. Nitridation for less than 5 h did not lead to the formation of the single wurtzite phase. In addition to the peaks assigned to the solid solution, some small peaks assigned to ZnO and $ZnGa_2O_4$ are observed in the nitridation products. The positions of the (100) and (101) diffraction peaks were successively shifted to higher angles (2θ) with increasing nitridation time, indicating that the obtained samples were not physical mixtures of GaN and ZnO phases but rather solid solutions of GaN and ZnO. The zinc and oxygen concentration in the solid solution thus decreased with reduction of the ZnO content and subsequent volatilization of zinc in the solid solution due to exposure to the reductive atmosphere during nitridation. This peak shift is reasonable, as the ionic radius of Zn^{2+} (0.74 Å) is larger than that of Ga^{3+} (0.61 Å).[13] In contrast, the position of the (002) diffraction peak did not undergo a shift, attributable to the smaller difference in *c*-axis lengths between GaN and ZnO compared to the difference in *a*-axis lengths.[14,15] The same tendency was confirmed by Rietveld analysis, using the computer program RIETAN-2000.[16] Figure 2 shows the relationship between refined lattice constants and zinc concentration (*x*) of $(Ga_{1-x}Zn_x)(N_{1-x}O_x)$. The *a*- and *c*-axis lengths of $(Ga_{1-x}Zn_x)(N_{1-x}O_x)$ increased almost linearly with increasing zinc concentration (*x*), although the *c*-axis length deviated slightly from this linear relationship due to the smaller difference in *c*-axis lengths between GaN and ZnO.[14,15]

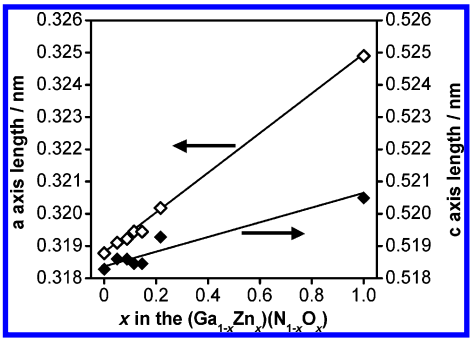

Figure 2. Relationship between lattice constants and zinc concentration (*x*) of the $(Ga_{1-x}Zn_x)(N_{1-x}O_x)$.

Figure 3 shows SEM images of the same samples. The particles of samples prepared by nitridation for less than 15 h were irregularly shaped, whereas those nitrided for longer periods became more regular and enlarged with nitridation time. This change in particle shape agrees well with the XRD measurements, which showed that the peaks became stronger and narrower with increasing nitridation time (Figure 1). These measurements reveal that the crystallization of the nitridation products proceeds gradually from 5 to 30 h during nitridation at 1123 K. TEM images and an electron diffraction pattern of the sample prepared by nitridation for 15 h are shown in Figure 4. The figure clearly reveals that the sample consisted of primary well-crystallized submicrometer-order particles with a wurtzite structure, as indicated by the lattice fringe and electron diffraction patterns.

3.2. X-ray Photoelectron Spectra. The valence state of Ga and Zn in the $(Ga_{1-x}Zn_x)(N_{1-x}O_x)$ solid solution was investigated by XPS. Figure 5 shows the XPS spectra for $Ga2p_{3/2}$, $Zn2p_{3/2}$, O1s, and N1s in $(Ga_{1-x}Zn_x)(N_{1-x}O_x)$ prepared at 1123 K over several periods. The data for GaN and ZnO are shown for comparison. The $Ga2p_{3/2}$ peaks for all prepared samples appear at almost the same positions as those for the GaN reference. The binding energy of $Ga2p_{3/2}$ in the GaN reference (1118.8

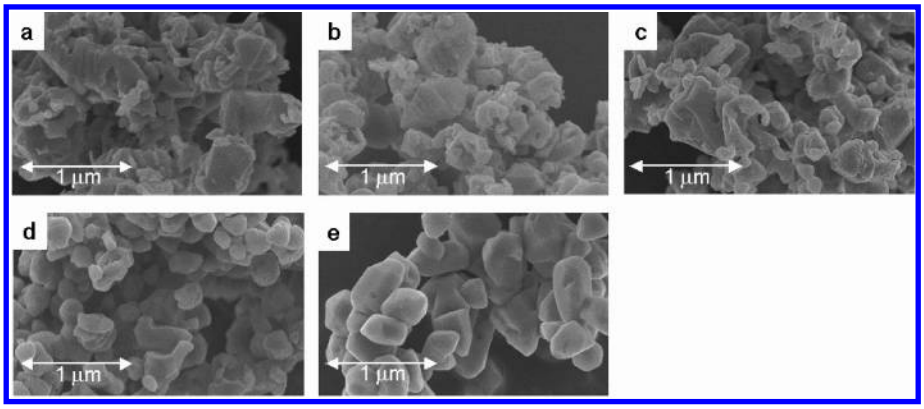

Figure 3. SEM images of obtained samples by nitriding a mixture of Ga_2O_3 and ZnO (molar ratio Zn/Ga = 1) under a flow of NH_3 at 1123 K for (a) 5, (b) 10, (c) 15, (d) 20, and (e) 30 h.

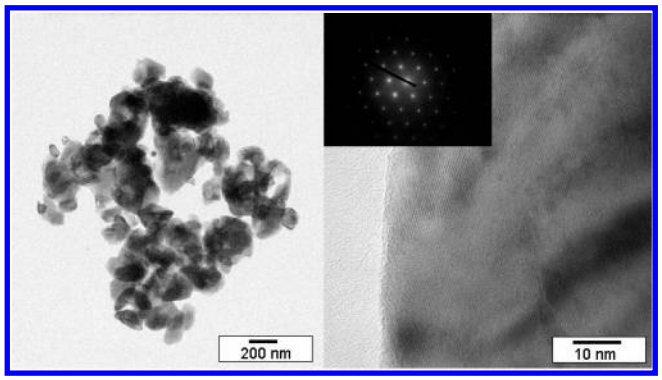

Figure 4. TEM images and an electron diffraction pattern of obtained sample by nitriding a mixture of Ga_2O_3 and ZnO (molar ratio Zn/Ga = 1) under a flow of NH_3 at 1123 K for 15 h.

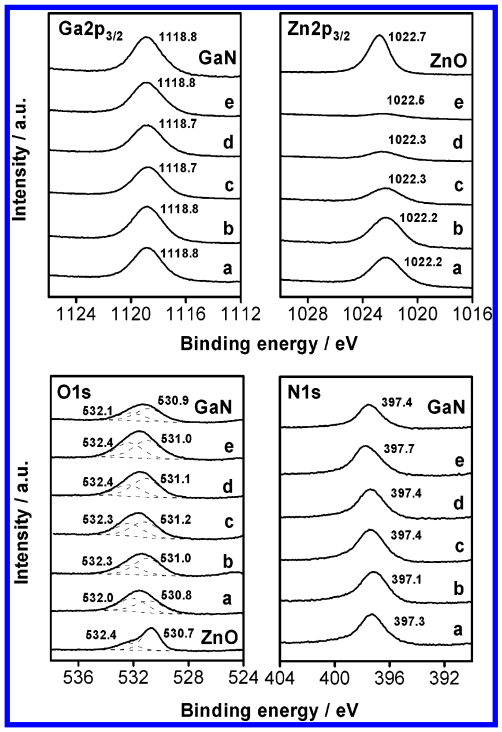

Figure 5. XPS spectra for Ga2p$_{3/2}$, Zn2p$_{3/2}$, O1s, and N1s of obtained samples by nitriding a mixture of Ga_2O_3 and ZnO (molar ratio Zn/Ga = 1) under a flow of NH_3 at 1123 K for (a) 5, (b) 10, (c) 15, (d) 20, and (e) 30 h.

eV) is higher than the reported values (1117.1 eV,[17] 1118.0 eV[18]) attributable to the oxygen species remaining on the surface as seen in the O1s spectra.[17] This result also indicates that oxygen species exist not only around Zn atoms but also around Ga atoms on the $(Ga_{1-x}Zn_x)(N_{1-x}O_x)$ surface. The Zn2p$_{3/2}$ peaks (1122.2−1122.5 eV) for all of the prepared samples appear at slightly lower energy positions than for the ZnO reference (1122.7 eV), considered to be due to the bond polarities of the Zn−O and Zn−N bonds and suggesting that the Zn−N bond is formed in $(Ga_{1-x}Zn_x)(N_{1-x}O_x)$. The intensity of the Zn2p$_{3/2}$ peak decreased with increasing nitridation time due to the reduction and volatilization of zinc in $(Ga_{1-x}Zn_x)(N_{1-x}O_x)$ during high-temperature nitridation. Judging from these results, Ga and Zn in $(Ga_{1-x}Zn_x)(N_{1-x}O_x)$ are almost entirely in the trivalent and divalent forms, respectively, regardless of nitridation time. The O1s peaks for all of the prepared samples can be resolved into 2 peaks (ca. 531.0 and 532.3 eV) assignable to lattice oxygen and surface OH groups, respectively. The positions of these peaks did not vary noticeably with nitridation time. Peaks assignable to lattice oxygen appeared at slightly higher positions in all of the present samples compared to the ZnO reference, indicating that oxygen atoms on the $(Ga_{1-x}Zn_x)(N_{1-x}O_x)$ surface possess less negative charge than those in ZnO. The N1s peaks for all samples appeared close to the position of the peak for the GaN reference (397.4 eV). These peak positions are close to that reported previously for N1s in GaN (397.3 eV,[18] 397.8 eV[19]), and clearly differ from that for N1s in Zn_3N_2 (395.8 eV).[20] This suggests that the nitrogen species on the $(Ga_{1-x}Zn_x)(N_{1-x}O_x)$ surface have an electronic state similar to that in GaN. This is considered to be reasonable by taking that the number of the Ga atoms existing on the $(Ga_{1-x}Zn_x)(N_{1-x}O_x)$ surface is larger than that of Zn atoms into account.

TABLE 1: Surface and Bulk Atomic Ratios of $(Ga_{1-x}Zn_x)(N_{1-x}O_x)$ Prepared by Nitriding for Several Time Periods

nitridation time[a] (h)	bulk Zn/Ga (O/N) ratio[b]	surface atomic ratio[c]		
		Zn/Ga	O/Ga	N/Ga
5	0.28	0.19	0.43	0.54
10	0.17	0.18	0.38	0.44
15	0.13	0.11	0.41	0.59
20	0.10	0.05	0.51	0.53
30	0.05	0.02	0.56	0.48

[a] Nitridation at 1123 K. [b] Estimated from EDX measurements. [c] Estimated from the XPS peak areas of Ga2p$_{3/2}$, Zn2p$_{3/2}$, O1s, and N1s.

3.3. Surface and Bulk Atomic Compositions. Table 1 shows the surface and bulk atomic compositions (Zn/Ga) for samples prepared by nitriding a mixture of Ga_2O_3 and ZnO (Zn/Ga = 1 by mole) at 1123 K for several periods. The surface atomic Zn/Ga ratios were estimated from the areas of the XPS peaks due to Zn2p$_{3/2}$ and Ga2p$_{3/2}$, and the bulk ratios were determined by EDX. It has been confirmed by previous elemental analyses

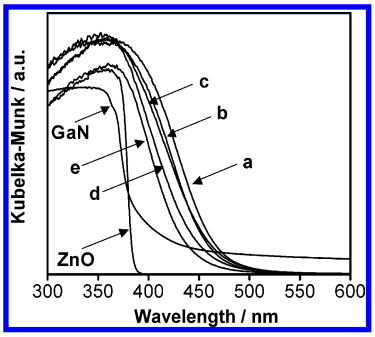

Figure 6. Diffuse reflectance spectra of obtained samples by nitriding a mixture of Ga_2O_3 and ZnO (molar ratio Zn/Ga = 1) under a flow of NH_3 at 1123 K for (a) 5, (b) 10, (c) 15, (d) 20, and (e) 30 h.

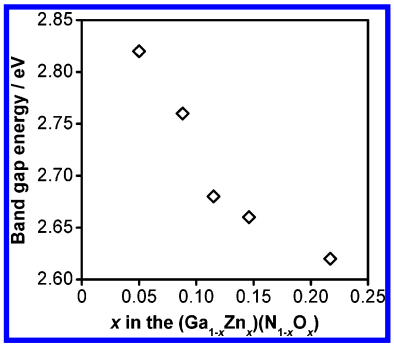

Figure 7. Relationship between band gap energies and zinc concentration (x) of the $(Ga_{1-x}Zn_x)(N_{1-x}O_x)$.

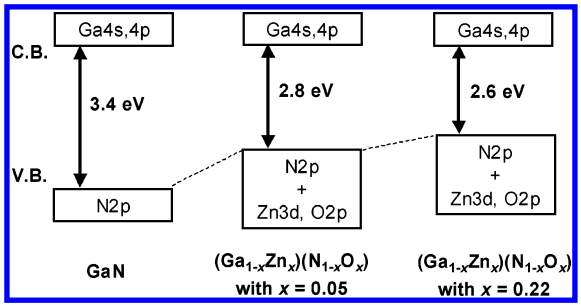

Figure 8. Schematic band structures of GaN and $(Ga_{1-x}Zn_x)(N_{1-x}O_x)$ with $x = 0.05-0.22$.

that the ratios of Ga to N and Zn to O are close to 1 and that the nitrogen and oxygen concentrations increase with the gallium and zinc concentrations.[9] Both the surface and bulk Zn/Ga ratios for the present samples were smaller than in the starting material (Zn/Ga = 1), and the ratios decreased with increasing nitridation time. This result agrees well with the XRD measurements (Figure 1). It is also clear that the volatilization of Zn tends to occur more easily on the surface of $(Ga_{1-x}Zn_x)(N_{1-x}O_x)$ than in the bulk. Note that under the present preparation conditions, the ZnO-only sample is easily reduced to a metal and volatilized at 1123 K.[21] Heating of a physical mixture of GaN and ZnO in N_2 or a vacuum did not lead to formation of the $(Ga_{1-x}Zn_x)(N_{1-x}O_x)$ solid solution. The detailed mechanism of $(Ga_{1-x}Zn_x)(N_{1-x}O_x)$ formation is currently under investigation. The surface O/Ga ratio estimated from the O1s peak due to lattice oxygen gradually increases with nitridation time, whereas the bulk oxygen concentration decreases with increasing nitridation time associated with the decrease in zinc concentration. This suggests that the oxygen species tend to remain at the $(Ga_{1-x}Zn_x)(N_{1-x}O_x)$ surface even after long periods of nitridation. It thus appears difficult to remove the remnant oxygen from $(Ga_{1-x}Zn_x)(N_{1-x}O_x)$ completely. No correlation between the surface N/Ga ratio and nitridation time was found for any of the present samples.

3.4. UV−Visible Diffuse Reflectance Spectra. Figure 6 shows the UV−visible diffuse reflectance spectra for $(Ga_{1-x}Zn_x)(N_{1-x}O_x)$ solid solutions prepared at 1123 K over several nitridation periods, along with the GaN and ZnO data for comparison. The absorption edges of $(Ga_{1-x}Zn_x)(N_{1-x}O_x)$ are located at longer wavelengths than those of GaN or ZnO, but shift to shorter wavelengths with increasing nitridation time. The band gap energy of the present samples is roughly estimated to be 2.6−2.8 eV based on the onsets of the diffuse reflectance spectra, which is substantially smaller than that for either GaN (3.4 eV) or ZnO (3.2 eV).

Our preliminary density functional theory (DFT) calculation revealed that the bottom of the conduction band for $(Ga_{1-x}Zn_x)(N_{1-x}O_x)$ is mainly composed of 4s and 4p orbitals of Ga, while the top of the valence band consists of N2p orbitals followed by Zn3d and O2p orbitals. It also indicated that the bottom of the conduction and the top of the valence bands for GaN are composed of 4s and 4p orbitals of Ga and N2p orbitals, respectively. For II−VI semiconductors, it has been pointed out that p−d repulsion shifts the valence-band maximum upward without affecting the conduction-band minimum.[22] This suggests that the presence of Zn3d and N2p electrons in the upper valence band of $(Ga_{1-x}Zn_x)(N_{1-x}O_x)$ provides p−d repulsion for the valence-band maximum, which results in narrowing the band gap. Figure 7 shows the relationship between band gap energies and zinc concentration (x) of $(Ga_{1-x}Zn_x)(N_{1-x}O_x)$. Obviously, the band gap energies of $(Ga_{1-x}Zn_x)(N_{1-x}O_x)$ decreased with increasing the zinc concentration, which corresponds to the result of DFT calculations. Thus, one possible explanation for the narrower band gap of $(Ga_{1-x}Zn_x)(N_{1-x}O_x)$ than GaN is a repulsion between N2p and Zn3d orbitals. Band structures of GaN and $(Ga_{1-x}Zn_x)(N_{1-x}O_x)$ are schematically depicted in Figure 8.

3.5. Dependence of Photocatalytic Activity on Nitridation Conditions. Figure 9 shows the dependence of the photocatalytic activity of RuO_2(5 wt %)-loaded $(Ga_{1-x}Zn_x)(N_{1-x}O_x)$ for overall water splitting under (A) UV and (B) visible light irradiation on the nitridation time of a mixture of Ga_2O_3 and ZnO (Zn/Ga = 1). BET surface areas are also shown. Stoichiometric H_2 and O_2 evolution was achieved for all samples, regardless of nitridation time. However, the rates of H_2 and O_2 evolution increased with nitridation time to a maximum at 15 h, beyond which the activity of the samples began to decrease. Under visible light, the dependence of the rate of gas evolution on the nitridation time was found to be similar to that under UV irradiation, with a maximum activity of 58 (H_2) and 29 $\mu mol \cdot h^{-1}$ (O_2) obtained for the sample nitrided for 15 h. In the range between 5 and 15 h of nitridation, where the largest increase in activity was obtained, the XRD peak became stronger and narrower (Figure 1). The increase in activity with nitridation time is therefore considered to be associated with the crystallization of $(Ga_{1-x}Zn_x)(N_{1-x}O_x)$, which reduces the number of defects acting as recombination centers between photogenerated electrons and holes. Nitridation for longer than 15 h had the effect of reducing the activity of the catalyst from the maximum value, which seems to be attributable to a loss of surface area with further crystallization. This result is consistent with the SEM observations (Figure 3). Many conventional metal-oxide photocatalysts have been reported to exhibit a decrease in photocatalytic activity with decreasing surface area of the catalyst.[10−12] This is caused by a decrease in the number of reaction sites on the catalyst surface and/or the coverage of the surface with excess amounts of cocatalyst. However, as shown in Figure 9, the activity of the $(Ga_{1-x}Zn_x)(N_{1-x}O_x)$ catalysts appears to be relatively robust with respect to surface area. The

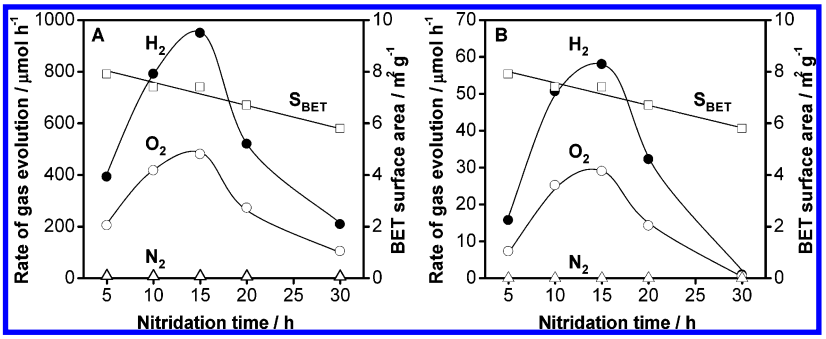

Figure 9. Dependence of the photocatalytic activity of RuO_2-loaded $(Ga_{1-x}Zn_x)(N_{1-x}O_x)$ for overall water splitting under (A) UV and (B) visible light irradiation on nitridation time. Catalyst (0.3 g), an aqueous solution adjusted to pH 3 by H_2SO_4 (390 mL); light source, high-pressure mercury lamp (450 W); inner irradiation-type reaction vessel made of Pyrex.

XPS and EDX analyses reveal that the zinc concentration in the $(Ga_{1-x}Zn_x)(N_{1-x}O_x)$ decreases with increasing nitridation time (Table 1). Under the present nitridation conditions, ZnO in the $(Ga_{1-x}Zn_x)(N_{1-x}O_x)$ is reduced to zinc metal and volatized to zinc vapor. The remnant oxygen species would be removed as H_2O, but are not completely removed (Table 1). The oxygen concentration in the bulk is also seen to decrease with decreasing zinc concentration. This situation results in vacancies at zinc sites in the catalyst surface, which may act as recombination centers between photogenerated electrons and holes. Kudo et al. reported that $ZnNb_2O_6$, a zinc-containing metal-oxide photocatalyst, exhibited the activity for overall water splitting under UV irradiation when loaded with NiO_x as a cocatalyst.[23] According to that study, the optimum reduction temperature for $Ni(NO_3)_2$-impregnated $ZnNb_2O_6$ is 573 K,[23] although the optimum reduction temperature for NiO_x-loaded photocatalysts has previously been reported to be 773 K.[10,11] It has been claimed that reductive treatment at high temperatures such as 773 K causes the catalyst surface to collapse due to the reduction and volatilization of zinc, indicating that zinc-containing materials have inherent weaknesses in reductive treatment. Accordingly, it is considered that the reason for the decrease in the photocatalytic activity of the present catalysts prepared by nitridation for longer than 15 h can be mainly attributed to the formation of zinc defects on the $(Ga_{1-x}Zn_x)(N_{1-x}O_x)$ surface. In addition, the difference of the composition between the bulk and the surface gradually enlarged with increasing nitridation time (Table 1), indicating that the electronic state of the surface is different from that of the bulk, which may hinder the prompt migration of photogenerated electrons and/or holes from the bulk to the surface of the catalyst.

Although nitridation of the mixture of Ga_2O_3 and ZnO at temperatures greater than 1173 K was also successful in producing $(Ga_{1-x}Zn_x)(N_{1-x}O_x)$, the final material was less active than the samples produced at 1123 K, regardless of nitridation time. This is considered to be attributable to the formation of zinc defects in the $(Ga_{1-x}Zn_x)(N_{1-x}O_x)$ surface at such high temperatures. Conversely, it was difficult to obtain a single phase of $(Ga_{1-x}Zn_x)(N_{1-x}O_x)$ at temperatures below 1073 K even for extended nitridation periods, probably due to the poor reactivity of starting materials with NH_3 gas at lower temperature. Thus, the optimal temperature for preparation of $(Ga_{1-x}Zn_x)(N_{1-x}O_x)$ is considered to be 1123 K.

A low level of N_2 evolution (ca. 5−10 μmol) was detected in the initial stage of the reaction (first 1−2 h) for all of the present samples. This is attributed to the oxidation of N^{3-} species near the $(Ga_{1-x}Zn_x)(N_{1-x}O_x)$ surface to N_2, as has been observed for other (oxy)nitride photocatalysts.[1−3] However, the production of N_2 is completely suppressed as the reaction progresses, and no changes in the XRD pattern of the catalyst were detected after the reaction. These results indicate that the $(Ga_{1-x}Zn_x)(N_{1-x}O_x)$ photocatalyst is essentially stable in the water splitting reaction.

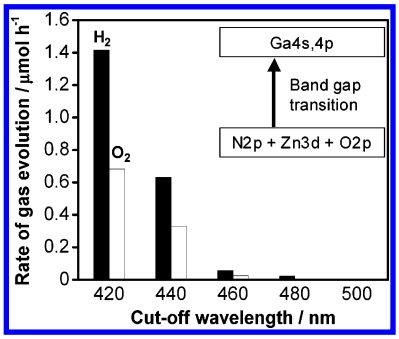

Figure 10. Dependence of the relative rates of H_2 and O_2 evolution on the cutoff wavelength of the incident light. Catalyst (0.3 g), an aqueous solution adjusted to pH 3 by H_2SO_4 (200 mL); light source, xenon lamp (300 W) attached with a cutoff filter; top irradiation-type reaction vessel made of Pyrex.

Figure 10 shows the dependence of the rate of H_2 and O_2 evolution on the wavelength of incident light. The H_2 and O_2 evolution rates both decrease as the cutoff wavelength is increased. The longest wavelength available for the water splitting reaction is 460 nm, corresponding to the absorption edge of the catalyst. This result clearly indicates that the reaction proceeded photocatalytically via the band gap transition from the valence band formed by N2p, Zn3d, and O2p hybridized orbitals to the conduction band formed by Ga4s,4p hybridized orbitals. The apparent quantum efficiency for overall water splitting at the optimized condition was calculated to be ca. 0.23%.

3.6. Effect of ZnO Ratio in Starting Material on Physical and Photocatalytic Properties. It is known that ZnO is reduced to metallic zinc upon exposure to a reducing atmosphere. The metallic zinc formed in this process converts to the liquid phase at temperatures between 700 and 1180 K,[21] and is thus considered to be useful as a flux under nitridation conditions. This behavior may indicate that the ratio of ZnO to Ga_2O_3 in the starting material for the preparation of $(Ga_{1-x}Zn_x)(N_{1-x}O_x)$ may affect the properties of the final catalyst.

We prepared $(Ga_{1-x}Zn_x)(N_{1-x}O_x)$ from the starting materials of a Ga_2O_3 and ZnO mixture in various Zn/Ga molar ratios. The nitridation condition of the starting materials was at 1123 K for 15 h, where the highest activity was obtained in the case of Zn/Ga = 1. Figures 11 and 12 show the XRD patterns and SEM images for these samples. Although no noticeable change in the XRD patterns can be detected (except for the Zn/Ga = 0.25 sample), the particle shapes became more regular with increasing Zn/Ga molar ratio, suggesting that the liquid zinc

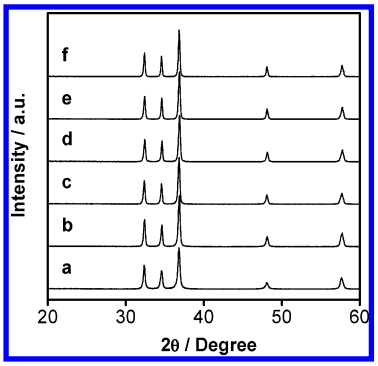

Figure 11. Powder XRD patterns of obtained samples by nitriding a mixture of Ga_2O_3 and ZnO at 1123 K for 15 h under a flow of NH_3 at 1123 K: Zn/Ga molar ratio in the starting mixture was (a) 0.25, (b) 0.5, (c) 0.75, (d) 1.0, (e) 1.25, and (f) 1.5.

metal produced by the reduction of ZnO under NH_3 flow at 1123 K facilitates formation of the $(Ga_{1-x}Zn_x)(N_{1-x}O_x)$ solid solution.

Table 2 shows the Zn/Ga atomic ratios and band gap energies estimated from the onset of the diffuse reflectance spectra for these samples. The Zn/Ga atomic ratios in the final catalysts are lower than those in the starting materials, indicating that most of the ZnO in the starting materials is reduced and volatilized during nitridation. It is reasonable that the band gap energies of these samples increased as the Zn/Ga atomic ratio in the final catalysts decreased, as mentioned above. It is noteworthy that the Zn/Ga atomic ratio tends to decrease gradually as the Zn/Ga molar ratio in the starting materials increases. The reason for this relationship is not clear at present, but is likely to be related to the mechanism by which the $(Ga_{1-x}Zn_x)(N_{1-x}O_x)$ solid solution is formed.

TABLE 2: The Ratios of Zn to Ga (Zn/Ga) and Band Gap Energies

Zn/Ga atomic ratio		
in starting materials	in products[a]	band gap energy[b] (eV)
0.25	0.14	2.69
0.5	0.14	2.70
0.75	0.13	2.68
1	0.13	2.68
1.25	0.11	2.74
1.5	0.09	2.81

[a] Estimated from EDX measurements. [b] Estimated from the onset of the diffuse reflectance spectra.

Figure 13 shows the dependence of the photocatalytic activity of RuO_2(5 wt %)-loaded $(Ga_{1-x}Zn_x)(N_{1-x}O_x)$ for overall water splitting under (A) UV and (B) visible light irradiation on the Zn/Ga molar ratio of the starting material. The rates of H_2 and O_2 evolution both increased with the Zn/Ga molar ratio to a maximum at Zn/Ga = 1, above which the evolution rates began to decline. The photocatalytic performances between UV and visible light were almost same. It appears that the increase in activity from Zn/Ga = 0.25 to 1 is mainly due to the crystallization of $(Ga_{1-x}Zn_x)(N_{1-x}O_x)$, which results in a decrease in the defect density on the catalyst surface, although the zinc concentration (x) in these low-ratio samples is similar (Table 2). Although the samples prepared at Zn/Ga = 1−1.5 are well crystallized (Figure 12), the activity of the catalysts decreased with increasing ratio of the starting materials, accompanied by a decrease in zinc concentration (Table 2). This relationship is consistent with the findings above in that the activity of $(Ga_{1-x}Zn_x)(N_{1-x}O_x)$ for overall water splitting depends strongly on the zinc concentration.

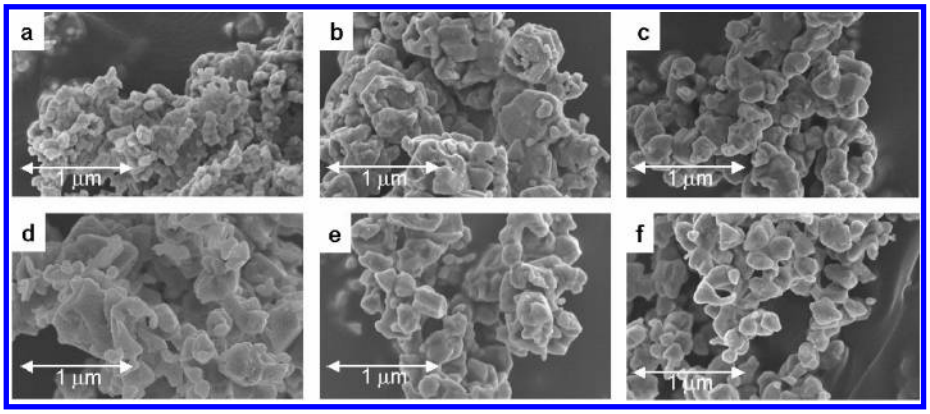

Figure 12. SEM images of obtained samples by nitriding a mixture of Ga_2O_3 and ZnO at 1123 K for 15 h under a flow of NH_3 at 1123 K: Zn/Ga molar ratio in the starting mixture was (a) 0.25, (b) 0.5, (c) 0.75, (d) 1.0, (e) 1.25, and (f) 1.5.

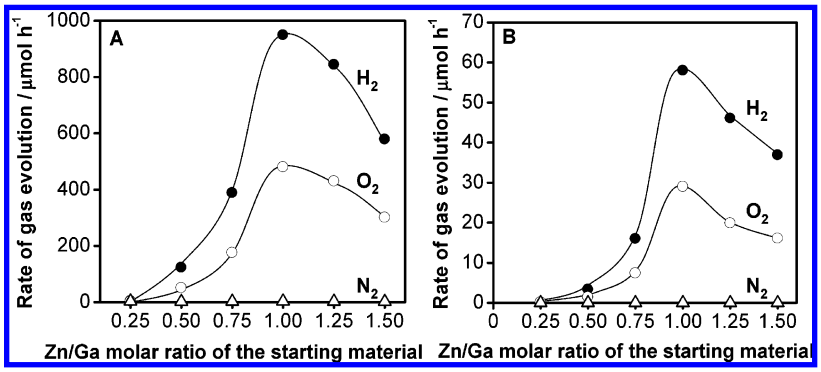

Figure 13. Dependence of the photocatalytic activity of RuO_2-loaded $(Ga_{1-x}Zn_x)(N_{1-x}O_x)$ for overall water splitting under (A) UV and (B) visible light irradiation on the Zn/Ga molar ratio of starting material. Catalyst (0.3 g), an aqueous solution adjusted to pH 3 by H_2SO_4 (390 mL); light source, high-pressure mercury lamp (450 W); inner irradiation-type reaction vessel made of Pyrex.

4. Conclusion

The $(Ga_{1-x}Zn_x)(N_{1-x}O_x)$ solid solution was investigated over the range of $x = 0.05-0.22$ as a photocatalyst for overall water splitting. The photocatalyst was prepared by nitriding a mixture of Ga_2O_3 and ZnO at 1123 K for 5−30 h under NH_3 flow, and the physical properties of the final material were confirmed to change with nitridation time. The highest activity for overall water splitting was obtained for the $(Ga_{1-x}Zn_x)(N_{1-x}O_x)$ sample with $x = 0.12$ and nitridation for 15 h. ZnO as a starting material was shown to play a role in promoting the crystallization of $(Ga_{1-x}Zn_x)(N_{1-x}O_x)$ and thus increasing the activity of the catalyst. Structural analyses revealed that the photocatalytic activity of $(Ga_{1-x}Zn_x)(N_{1-x}O_x)$ for overall water splitting depends heavily on the crystallinity and composition of the material, where the zinc concentration in both the starting material and the final catalyst is of particular importance.

Acknowledgment. This work was supported by the Solution Oriented Research for Science and Technology (SORST) program of the Japan Science and Technology (JST) Corporation and the 21st Century Center of Excellence (COE) program of the Ministry of Education, Culture, Sports, Science and Technology of Japan.

References and Notes

(1) Hitoki, G.; Takata, T.; Kondo, J. N.; Hara, M.; Kobayashi, H.; Domen, K. *Chem. Commun.* **2002**, 1698.

(2) Hitoki, G.; Ishikawa, A.; Takata, T.; Kondo, J. N.; Hara, M.; Domen, K. *Chem. Lett.* **2002**, *31*, 736.

(3) Kasahara, A.; Nukumizu, K.; Hitoki, G.; Takata, T.; Kondo, J. N.; Hara, M.; Kobayashi, H.; Domen, K. *J. Phys. Chem. A* **2002**, *106*, 6750.

(4) Ishikawa, A.; Takata, T.; Kondo, J. N.; Hara, M.; Kobayashi, H.; Domen, K. *J. Am. Chem. Soc.* **2002**, *124*, 13547.

(5) Ishikawa, A.; Takata, T.; Matsumura, T.; Kondo, J. N.; Hara, M.; Kobayashi, H.; Domen, K. *J. Phys. Chem. B* **2004**, *108*, 2637.

(6) Kato, H.; Kudo, A. *J. Phys. Chem. B* **2002**, *106*, 5029.

(7) Konta, R.; Ishii, T.; Kato, H.; Kudo, A. *J. Phys. Chem. B* **2004**, *108*, 8992.

(8) Sato, J.; Saito, N.; Yamada, Y.; Maeda, K.; Takata, T.; Kondo, J. N.; Hara, M.; Kobayashi, H.; Domen, K.; Inoue, Y. *J. Am. Chem. Soc.* **2005**, *127*, 4150.

(9) Maeda, K.; Takata, T.; Hara, M.; Saito, N.; Inoue, Y.; Kobayashi, H.; Domen, K. *J. Am. Chem. Soc.* **2005**, *127*, 8286.

(10) Kudo, A.; Tanaka, A.; Domen, K.; Onishi, T. *J. Catal.* **1988**, *111*, 296.

(11) Ikeda, S.; Hara, M.; Kondo, J. N.; Domen, K.; Takahashi, H.; Okubo, T.; Kakihana, M. *Chem. Mater.* **1998**, *10*, 72.

(12) Sato, J.; Kobayashi, H.; Ikarashi, K.; Saito, N.; Nishiyama, H.; Inoue, Y. *J. Phys. Chem. B* **2004**, *108*, 4369.

(13) Shannon, R. D. *Acta Crystallogr., Sect. A* **1976**, *32*, 751.

(14) Suhulz, H.; Thiemann, K. H. *Solid State Commun.* **1977**, *23*, 815.

(15) Garcia-Martinez, O.; Rojas, R. M.; Vila, E.; Martin de Vidales, J. L. *Solid State Ionics* **1997**, *63*, 442.

(16) Izumi, F.; Ikeda, T. *Mater. Sci. Forum* **2000**, *321−324*, 198.

(17) Tran, N. H.; Houschuh, W. J.; Lamb, R. N.; Lai, L. J.; Yang, Y. W. *J. Phys. Chem. B* **2003**, *107*, 9256.

(18) Dinescu, M.; Verardi, P.; Boulmer-Leborgne, C.; Gerardi, C.; Mirenghi, L.; Sandu, V. *Appl. Surf. Sci.* **1998**, *127−129*, 559.

(19) Yang, Y. G.; Ma, H. L.; Xue, C. S.; Hao, X. T.; Zhuang, H. Z.; Ma, J. *Phys. B* **2003**, *325*, 230.

(20) Futsuhara, M.; Yoshioka, K.; Takai, O. *Thin Solid Films* **1998**, *322*, 274.

(21) Lide, D. R. *Handbook of Chemistry and Physics*, 83rd ed.; CRC Press: Boca Raton, FL, 2002.

(22) Wei, S. H.; Zunger, A. *Phys. Rev. B* **1988**, *37*, 8958.

(23) Kudo, A.; Nakagawa, S.; Kato, H. *Chem. Lett.* **1999**, *28*, 1197.